



# Gain-of-function mutations of the V2 vasopressin receptor in nephrogenic syndrome of inappropriate antidiuresis (NSIAD): a cell-based assay to assess constitutive water reabsorption

Marianna Ranieri<sup>1</sup> · Grazia Tamma<sup>1,2</sup> · Tommaso Pellegrino<sup>1</sup> · Vanessa Vezzi<sup>3</sup> · Caterina Ambrosio<sup>3</sup> · Cristina Grò<sup>3</sup> · Annarita Di Mise<sup>1</sup> · Tommaso Costa<sup>3</sup> · Giovanna Valenti<sup>1,2,4</sup> · Susanna Cotecchia<sup>1</sup>

Received: 12 April 2019 / Revised: 28 August 2019 / Accepted: 29 August 2019 / Published online: 5 September 2019  
© Springer-Verlag GmbH Germany, part of Springer Nature 2019

## Abstract

Nephrogenic syndrome of inappropriate antidiuresis (NSIAD) is a recently identified chromosome X-linked disease associated with gain-of-function mutations of the V2 vasopressin receptor (V2R), a G-protein-coupled receptor. It is characterized by inability to excrete a free water load, hyponatremia, and undetectable vasopressin-circulating levels. Hyponatremia can be quite severe in affected male children. To gain a deeper insight into the functional properties of the V2R active mutants and how they might translate into the pathological outcome of NSIAD, in this study, we have expressed the wild-type V2R and three constitutively active V2R mutants associated with NSIAD (R137L, R137C, and the F229V) in MCD4 cells, a cell line derived from renal mouse collecting duct, stably expressing the vasopressin-sensitive water channel aquaporin-2 (AQP2). Our findings indicate that in cells expressing each active mutant, AQP2 was constitutively localized to the apical plasma membrane in the absence of vasopressin stimulation. In line with these observations, under basal conditions, osmotic water permeability in cells expressing the constitutively active mutants was significantly higher compared to that of cells expressing the wild-type V2R. Our findings demonstrate a direct link between activating mutations of the V2R and the perturbation of water balance in NSIAD. In addition, this study provides a useful cell-based assay system to assess the functional consequences of newly discovered activating mutations of the V2R on water permeability in kidney cells and to screen the effect of drugs on the mutated receptors.

**Keywords** V2 receptor · AQP2 · NSIAD

## Introduction

In most mammals, including humans, the maintenance of water balance is under the control of the antidiuretic hormone arginine vasopressin (AVP). AVP is secreted into the

circulation by the posterior pituitary gland, in response to increased serum osmolality or decreased blood volume.

In the kidney, AVP binds to the V2 vasopressin (V2R) receptor belonging to the superfamily of G-protein-coupled receptors (GPCRs). V2 receptors expressed in the basolateral membranes of the collecting duct epithelial cells activate the Gs protein thus increasing intracellular cAMP [1]. It is well established that binding of AVP to the V2 receptors leads to protein kinase A-mediated translocation of aquaporin-2 (AQP2) water-channel proteins to the apical membrane thus promoting water reabsorption (reviewed in [2]). However, recent lines of evidence suggest multiple mechanisms involved in V2-mediated increased water reabsorption [3–5].

Loss-of-function mutations of both V2R and AQP2 are associated with congenital nephrogenic diabetes insipidus (NDI), a rare genetic disorder, which can be quite severe in infants, characterized by a failure to concentrate urine (despite normal or elevated levels of AVP), polyuria, polydipsia, and hypernatremia [6–8].

---

✉ Giovanna Valenti  
giovanna.valenti@uniba.it

✉ Susanna Cotecchia  
susanna.cotecchia@uniba.it

<sup>1</sup> Department of Biosciences, Biotechnologies and Biopharmaceutics, University of Bari, 70125 Bari, Italy

<sup>2</sup> Istituto Nazionale di Biostrutture e Biosistemi, 00136 Rome, Italy

<sup>3</sup> Department of Pharmacology, Istituto Superiore di Sanità, 00161 Rome, Italy

<sup>4</sup> Center of Excellence in Comparative Genomics (CEGBA), University of Bari, 70125 Bari, Italy

Mutations of the V2R cause the X-linked form of congenital NDI, whereas mutations in the gene encoding aquaporin-2 are responsible for both the autosomal recessive and autosomal dominant forms. At present, more than 180 loss-of-function mutations in the V2R have been described in association with X-linked NDI.

In 2005, gain-of-function mutations of the V2R have been discovered in two unrelated infants affected by hyponatremia with undetectable levels of circulating AVP [9]. Inappropriate antidiuresis is the most common cause of hyponatremia and is characterized by inability to excrete a free water load, hyponatremia, hypo-osmolality, and natriuresis. The most common clinical entity of inappropriate antidiuresis is the idiopathic syndrome of inappropriate antidiuretic hormone secretion (SIADH) which is linked to hypersecretion of AVP [10]. However, 10–20% of patients with inappropriate antidiuresis display low or undetectable AVP circulating levels. The identification of gain-of-function mutations of the V2R in those two infants with severe hyponatremia led to the definition of nephrogenic syndrome of inappropriate antidiuresis (NSIAD) as a new clinical entity of inappropriate antidiuresis which, in contrast to SIADH, is characterized by low or undetectable levels of AVP [8].

In the first two cases of NSIAD described above, activating mutations of the V2R have been found at residue R137 belonging to the highly conserved DRY/H sequence at the cytosolic end of helix 3 of GPCRs which plays a crucial role in the activation process of the receptors. Substitution of R137 to cysteine or leucine (R137C and R137L) results in constitutive activation of the V2R associated with NSIAD. Interestingly, conversion of R137 to histidine (R137H) is a well-known loss-of-function mutation associated with NDI leading to water loss and inability to concentrate urine [11]. Thus, mutations of the same amino acid of the V2R, R137, can have opposite clinical outcomes.

A novel activating mutation, F229V at the cytosolic end of helix 5, was found in the V2R of a 3-month-old severely affected male infant [12]. More recently, two other activating mutations have been described in patients with hyponatremia: I130N and L312S in the third and seventh transmembrane helix, respectively [13, 14]. Thus, constitutively activating mutations of the tubular V2R, which can activate signaling in the absence of hormonal stimulation, seem to be the most probable mechanism underlying increased free water reabsorption in NSIAD.

Standard treatments of NSIAD consist of fluid restriction and urea to increase urine osmolality. However, fluid restriction poses a challenge especially in infancy because it is associated with limited calorie intake. The ideal treatment would be represented by V2R antagonists with properties of “inverse agonists,” but two of them, tolvaptan and satavaptan, had no efficacy in patients carrying mutations of R137 [15]. In contrast, both inverse agonists could almost entirely abolish the

constitutive activity of the F229V, I130N mutants, and L312S in vitro, thus suggesting that they could be effective on patients carrying these mutations [12–14].

Some of the molecular properties of the constitutively active V2R mutants found in NSIAD have been investigated in previous studies [9, 12, 16, 17], but several questions remain open on their role in the pathogenesis of the disease as well as on the most effective treatments.

So far, for all V2R mutants, constitutive activity was mainly described as their ability to increase basal cAMP levels in HEK-293 or COS cells expressing the receptors. Considering the degree of constitutive activity on cAMP levels and other biochemical properties, the V2R mutants associated with NSIAD can be divided in two groups with quite different features. In group 1, including F229V, I130N and L312S mutant receptors display quite normal cell surface expression, no increased basal interaction with  $\beta$ -arrestin, and high constitutive activity on cAMP accumulation which can be almost entirely abolished by the inverse agonists tolvaptan and satavaptan [12–14]. In group 2, formed by R137C and R137L, the mutated receptors display weak constitutive activity on cAMP levels, constitutive  $\beta$ -arrestin recruitment, and decreased cell surface expression [12, 17, 18]. In addition, the small constitutive activity of R137C and R137L mutants on cAMP levels is not inhibited by inverse agonists.

To gain a deeper insight into the functional implications of the V2R activating mutations and how they might translate into the pathological outcome of NSIAD, in this study, we have expressed the wild-type V2R and constitutively active V2R mutants, of both groups 1 and 2, in cells from the kidney collecting duct stably expressing human AQP2 (MCD4 cells), which represent the physiological environment where the receptors are expressed. In these cells, we have compared the ability of the wild-type and mutated V2 receptors to affect some functional parameters of AQP2 including its translocation to the apical membrane and AQP-mediated water reabsorption.

## Results

### Expression of V2 receptors in MCD4 cells

To explore the effect of the functional expression of different mutations of the V2R on water transport, wild-type and mutated V2 receptors were stably expressed in the MCD4 cells, a cell line derived from renal mouse collecting duct cells with no significant levels of endogenous V2R, in which human AQP2 has been overexpressed [19]. Cells were stably transfected using a retroviral vector encoding the wild-type V2R, the inactive R137H mutant associated with NDI, two active mutants of group 1 (R137L and R137C), or one active mutant of group 2 (F229V) mutations associated with NSIAD. The

cDNA of receptors carried a c-Myc sequence in the N-terminal portion for immunodetection and the Renilla luciferase cDNA within the C terminus.

Receptor expression was assessed using different approaches including western blotting, cell surface ELISA, and confocal microscopy.

As shown in Fig. 1 a, western blotting on plasma membrane-enriched preparations from transfected cells, using monoclonal anti-Myc antibodies, revealed that all receptors were expressed displaying a similar migration pattern characterized by two main bands, at  $\approx 80$  and  $\approx 72$  kDa. The predominant band of  $\approx 80$  kDa, observed for all receptors, corresponds well to the size expected for the mature V2R ( $\approx 45$  kDa [16]) fused to Renilla luciferase ( $\approx 35$  kDa). Considering the intensity of both protein bands, the expression level of all mutated receptors was overall lower compared to that of the wild-type V2R with the inactive R137H showing the weakest expression.

Surface and total expression of the V2 receptors in MCD4 cells were measured by cell-based ELISA and Renilla

luciferase luminescence, respectively, as described in the “Materials and methods.” As shown in Fig. 1 b, in which levels in cells expressing the mutated receptors are normalized to those of cells expressing the wild-type V2R, cell surface expression could be detected for all receptor mutants. However, the level of cell surface receptors of the receptor mutants was more than 50% lower compared to that of the wild-type V2R (R137L  $28.1 \pm 8.0\%$ ; R137C  $41.7 \pm 5.8\%$ ; F229V  $25.8 \pm 3.3\%$  vs V2R-wt), the lowest level being observed for the inactive R137H mutant (R137H  $15.9 \pm 2.1\%$  vs V2R-wt).

Whereas the results on expression of the R137 mutants are in good agreement with those reported by other groups expressing these receptors in different cell lines [16], cell surface expression of the F229V mutant is lower (30% of the wild type) compared to that reported in a previous study (80% of the wild type) [12]. This is, probably, due to the fact that total expression of the F229V in our cell system is smaller than that of the wild-type V2R, as demonstrated by the low level of luminescence measured (Fig. 1b).

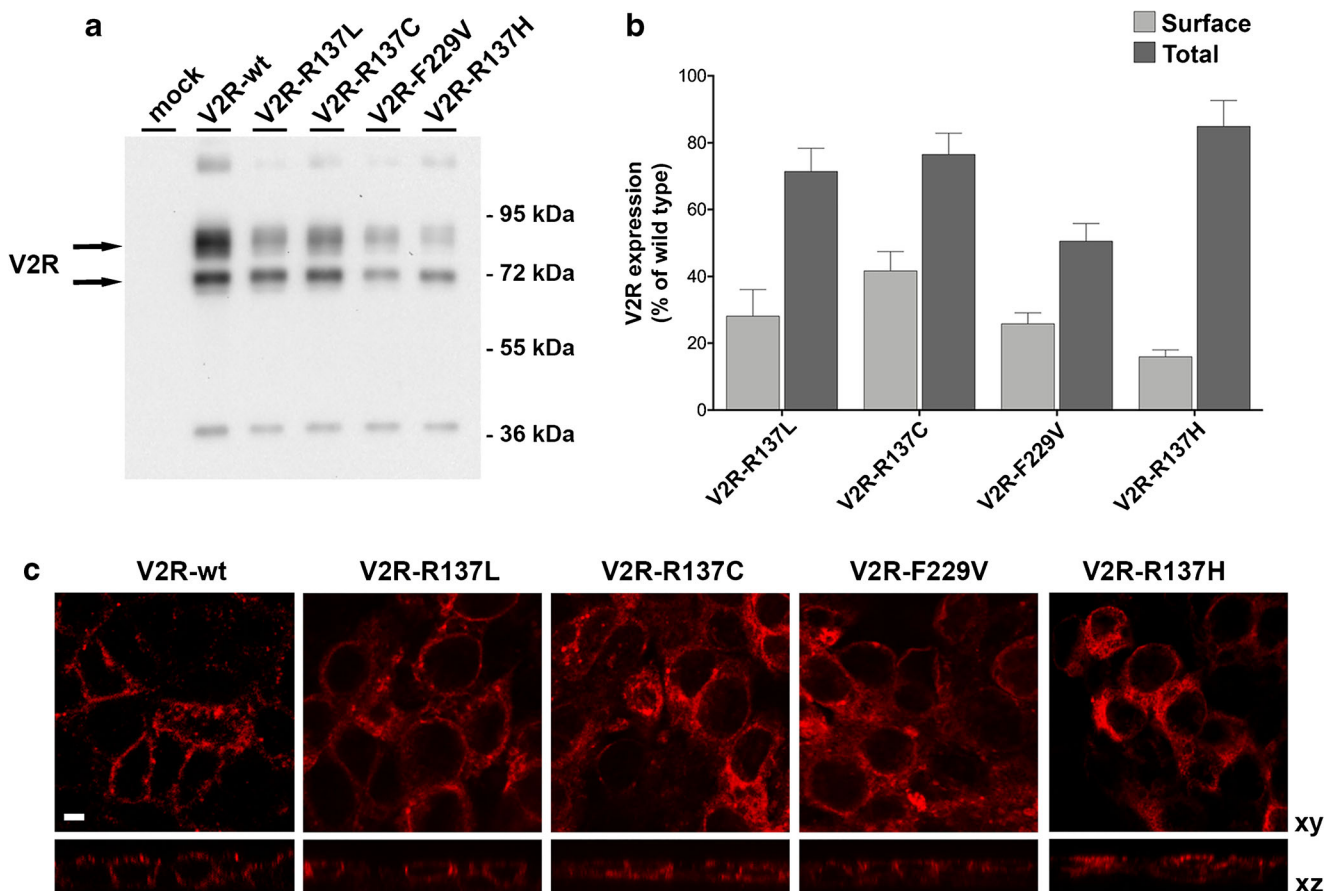


**Fig. 1** Expression of V2 receptors in MCD4 cells. **a** Western blotting on plasma membrane-enriched preparations ( $21,000\times g$ ) from transfected MCD4 cells, using monoclonal anti-Myc antibodies and revealing two main bands, at  $\approx 80$  and  $\approx 72$  kDa. **b** Surface and total expression of the V2 receptors in MCD4 cells measured by cell-based ELISA and Renilla luciferase luminescence. The data, expressed as percentage of the level in

cell expressing wild-type V2R, are means ( $\pm$  s.e.m.) of 5 experiments. **c** Confocal immunofluorescence analysis of wild-type (V2R-wt) and mutated receptors (V2R-R137L/C/H, V2R-F229V) using fluorescent monoclonal anti-Myc antibodies in MCD4 cells grown on filters. Immunostaining was visualized in xy apical confocal plan (upper panel) and in xz confocal plan (lower panel) (scale bar  $5 \mu\text{m}$ )

To assess the cellular distribution of the V2R mutants, we performed confocal microscopy on MCD4 cells expressing the wild-type and mutated receptors using fluorescent monoclonal anti-Myc antibodies. Cells were grown on permeable filters to allow their polarization and images were taken on both  $xy$  and  $xz$  axes.

As shown in Fig. 1 c ( $xy$  image), in basal conditions, the wild-type V2R was mainly localized at the cell surface as indicated by the sharp fluorescence along the perimeter of the cells. The F229V mutant displayed a pattern similar to that of the wild-type V2R, but fluorescence was a bit weaker in agreement with the lower level of F229V expression as observed in panels a and b. In cells expressing either the active R137L and R137C mutants or the inactive R137H, intracellular fluorescence was more pronounced compared to that of the wild-type V2R with both a punctuated and reticular pattern.

As can be seen in the  $xz$  images of Fig. 1, the wild-type V2R is localized at both the basolateral and apical membranes. The apical localization of the receptor might be due either to receptor overexpression or to an incomplete polarization of the cells. Also for the active mutants, R137L, R137C, and F229V, in addition to the basolateral fluorescence, a faint signal could be detected on the apical side. In contrast, for the inactive R137H mutant, the fluorescence signal was rather diffuse through the cytoplasm suggesting that the receptor is mainly intracellular.

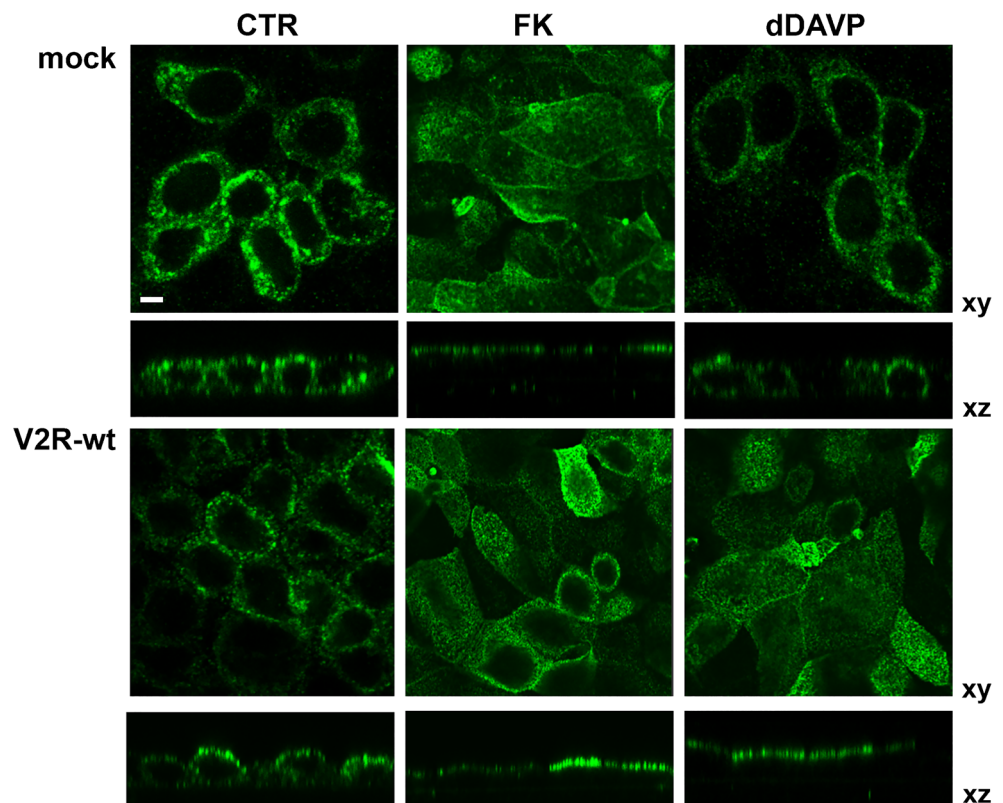
Overall, these findings on MCD4 cells are consistent with those from previous studies in other cell lines indicating that both active and inactive receptors carrying mutation of R137 display increased retention in the intracellular compartments probably due to both misfolding and constitutive endocytosis [14, 16].

### AQP2 localization and water transport in cells expressing the V2 receptors

To investigate the physiological effects of the V2R constitutively active mutants on water homeostasis, AQP2 localization and water permeability were investigated in MCD4 cells expressing the wild-type or mutated receptors. In agreement with previous findings, confocal microscopy in cells grown on permeable filters expressing the wild-type V2R revealed that, under basal conditions, AQP2 staining was mainly localized in intracellular vesicles (Fig. 2). As clearly visible in the  $xz$  images of Fig. 2, stimulation of cells with either forskolin (FK) or desmopressin (dDAVP) resulted in marked redistribution of AQP2 to the apical plasma membrane. This finding supports the paradigm that activation of V2R in kidney cells triggers AQP2 translocation to the plasma membrane which contributes to increased water reabsorption.

Confocal analysis in MCD4 cells expressing each constitutively active mutant, R137L, R137C, or F229V, revealed that, under basal conditions, staining of AQP2 in the apical

**Fig. 2** AQP2 translocation in cells expressing the wild-type V2R. Confocal immunofluorescence analysis of AQP2 localization in MCD4 cells grown on filters not expressing recombinant receptors (mock) or expressing the wild-type V2R (V2R-wt), in resting conditions (CTR), after forskolin (FK) stimulation or after desmopressin (dDAVP) stimulation, as described in the “Materials and methods.” Immunostaining was visualized in  $xy$  apical confocal plan (upper panels) and in  $xz$  confocal plan (lower panels) (scale bar 5  $\mu$ m)





plasma membrane was more pronounced compared to that of cells expressing the wild-type V2R (Fig. 3a). AQP2 fluorescence at the apical membrane was much sharper for the F229V mutant with respect to R137C or R137L receptors. In contrast, in cells expressing the inactive R137H mutant, AQP2 was mainly localized in intracellular vesicles with no clear staining at the apical membrane. These findings provide strong evidence that, in MDC4 cells expressing constitutively active V2R mutants, AQP2 is constitutively localized, at different extent, at the apical membrane probably because of agonist-independent receptor signaling.

To quantify the insertion of AQP2 into the apical plasma membrane, we performed cell surface biotinylation experiments of AQP2 in polarized MCD4 cells expressing the various receptors (Fig. 3b). Compared to cells expressing the wild-type V2R ( $1.00 \pm 0.17$  a.u.), cell surface expression of AQP2 was significantly higher in cells expressing the active R137L ( $1.58 \pm 0.03$  a.u.), R137C ( $1.56 \pm 0.07$  a.u.), and F229V ( $2.08 \pm 0.22$  a.u.) mutants, the last displaying the highest value. In contrast, in cells expressing the inactive

R137H mutant, AQP2 abundance at the cell surface was even significantly lower ( $0.34 \pm 0.04$  a.u.) than in cells expressing the wild-type V2R. This seems to indicate a certain degree of constitutive activity also for the wild-type V2R overexpressed in MCD4 cells.

To assess the functional outcome of AQP2 translocation, the osmotic water permeability was measured in MCD4 cells expressing either the wild-type V2R or different receptor mutants, as previously described [5]. As shown in Fig. 4, in cells expressing the constitutive active mutants, the temporal osmotic response (indicated as  $1/\tau$ ) was significantly higher (R137L  $145.8 \pm 4.6\%$ ; R137C  $144.4 \pm 4.3\%$ ; F229V  $167.7 \pm 4.6\%$ ;  $p < 0.05$ ) compared with that of cells expressing the wild-type V2R ( $100.0 \pm 2.6\%$ ), indicating increased water permeability in the absence of dDAVP stimulation. The increase in water permeability correlates with AQP2 translocation to the apical membrane being greater in cells expressing the F229V mutant compared to cells expressing either the R137L or R137C receptor. In contrast, the value of the temporal osmotic response in cells expressing the inactive R137H

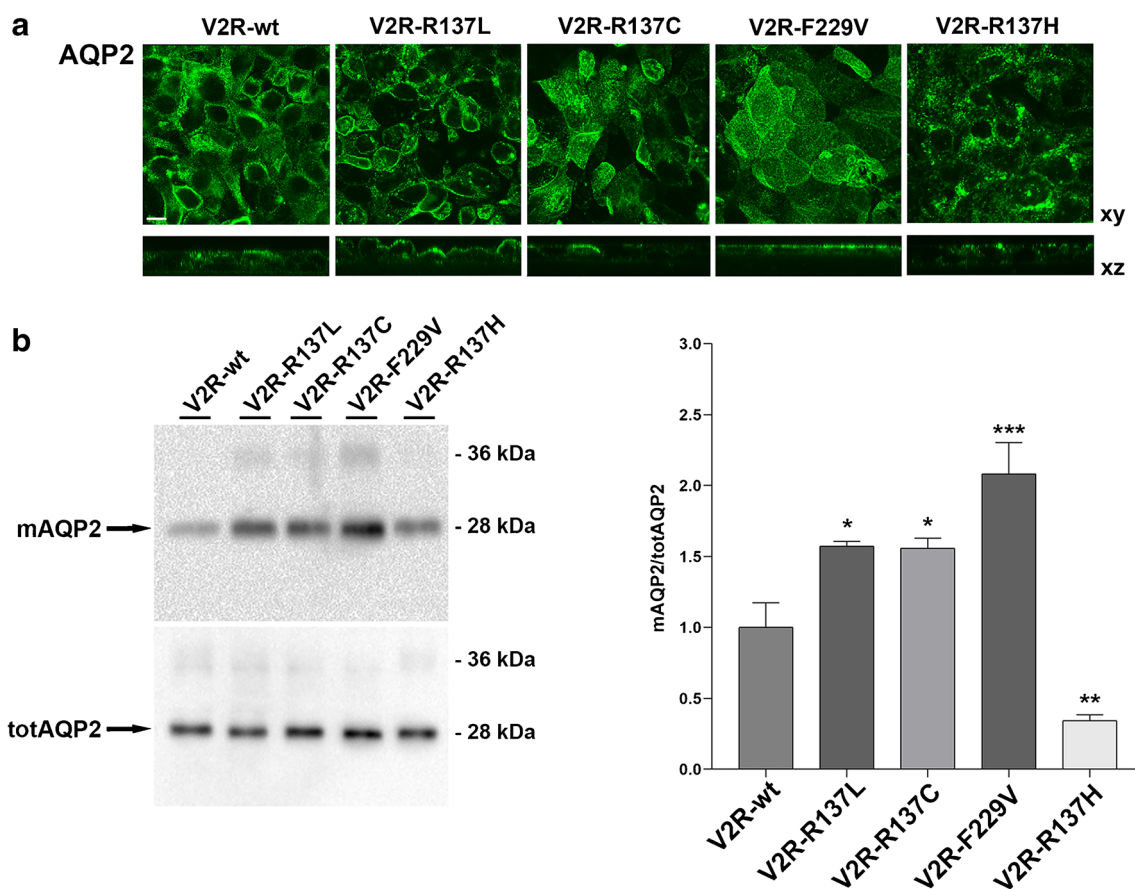


**Fig. 3** AQP2 translocation in cells expressing the wild-type and mutated V2R. MCD4 cells expressing the wild-type V2R; the constitutively active R137L, R137C, or F229V; and the inactive R137H were grown on filters. **a** Confocal analysis was performed in basal conditions using anti-AQP2 antibody. Immunostaining was visualized in *xy* apical confocal plan (upper panel) and in *xz* confocal plan (lower panel) (scale bar 5  $\mu$ m). **b**

Biotinylation experiments were performed as described in the “Materials and methods.” Densitometric analysis of bands of AQP2 biotinylated at the apical membrane (mAQP2) normalized to the total AQP2 bands (totAQP2) is shown in the histogram. The data, normalized to the level in cell expressing wild-type V2R, are means ( $\pm$  s.e.m.) of 5 experiments (\* $p < 0.05$ ; \*\* $p < 0.01$ ; \*\*\* $p < 0.001$  vs V2R-wt)

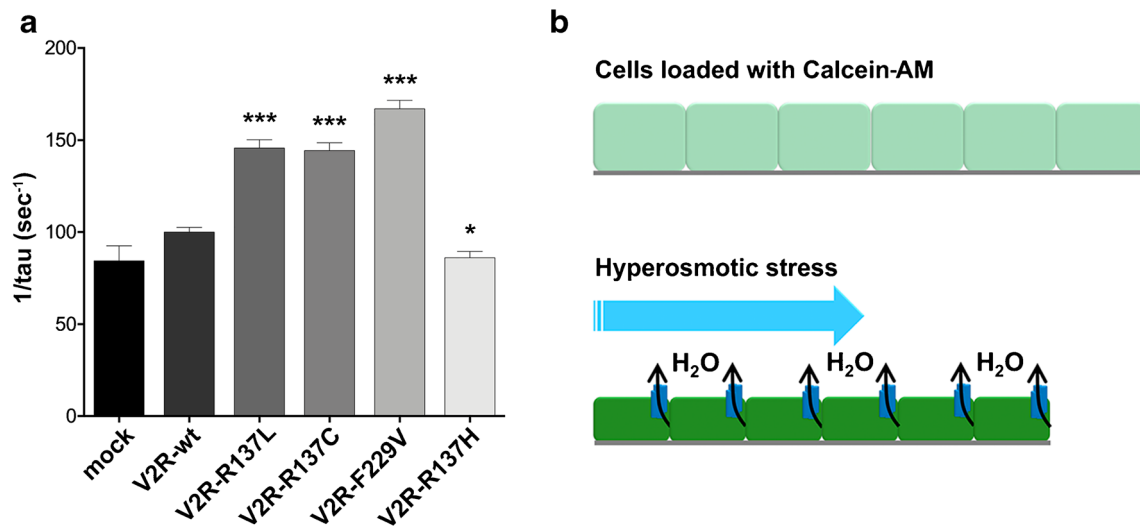


**Fig. 4** Water permeability in cells expressing the wild-type and mutated V2R. **a** Osmotic permeability studies in MCD4 mock cells (not expressing recombinant receptors) or expressing the wild-type V2R; the constitutive active R137L, R137C, and F229V; and the inactive R137H were performed as reported in the “Materials and methods.” The temporal osmotic response is indicated as  $1/\tau$  ( $\text{s}^{-1}$ ). The data, expressed as percentage of the level in cell expressing wild-type V2R, are means ( $\pm$  s.e.m.) of

5 experiments ( $*p < 0.05$ ;  $***p < 0.001$  vs V2R-wt). **b** Schematic model showing the water permeability assay in MCD4 cells loaded with Calcein-AM dye. Exposure to a hyperosmotic solution causes water efflux with a consequent cell shrinkage resulting in Calcein-AM increased concentration and self-quenching. The speed of decrease in fluorescence intensity is proportional to the speed of water efflux and, indirectly, to the water permeability through AQP2 water channels

mutant was slightly but significantly decreased ( $86.04 \pm 3.4\%$ ;  $p < 0.05$ ) with respect to cells expressing the wild-type V2R. The osmotic water permeability of mock cells was not significantly different from V2R-wt expressing cells. These findings provide evidence of a direct link between constitutively activating mutations of the V2R and increased water reabsorption in kidney cells under basal conditions which might be responsible for the clinical outcome observed in patients suffering from NSIAD.

### cAMP levels in cells expressing the V2 receptors

It is well established that the effect of V2R on increased AQP2 translocation to the plasma membrane and water reabsorption is, at least in part, mediated by the cAMP–PKA pathway (reported in [3, 20–24]). Therefore, to assess the role of cAMP in constitutive activation of water reabsorption in MCD4 cells expressing the active V2R mutants, cAMP was measured in whole cells.

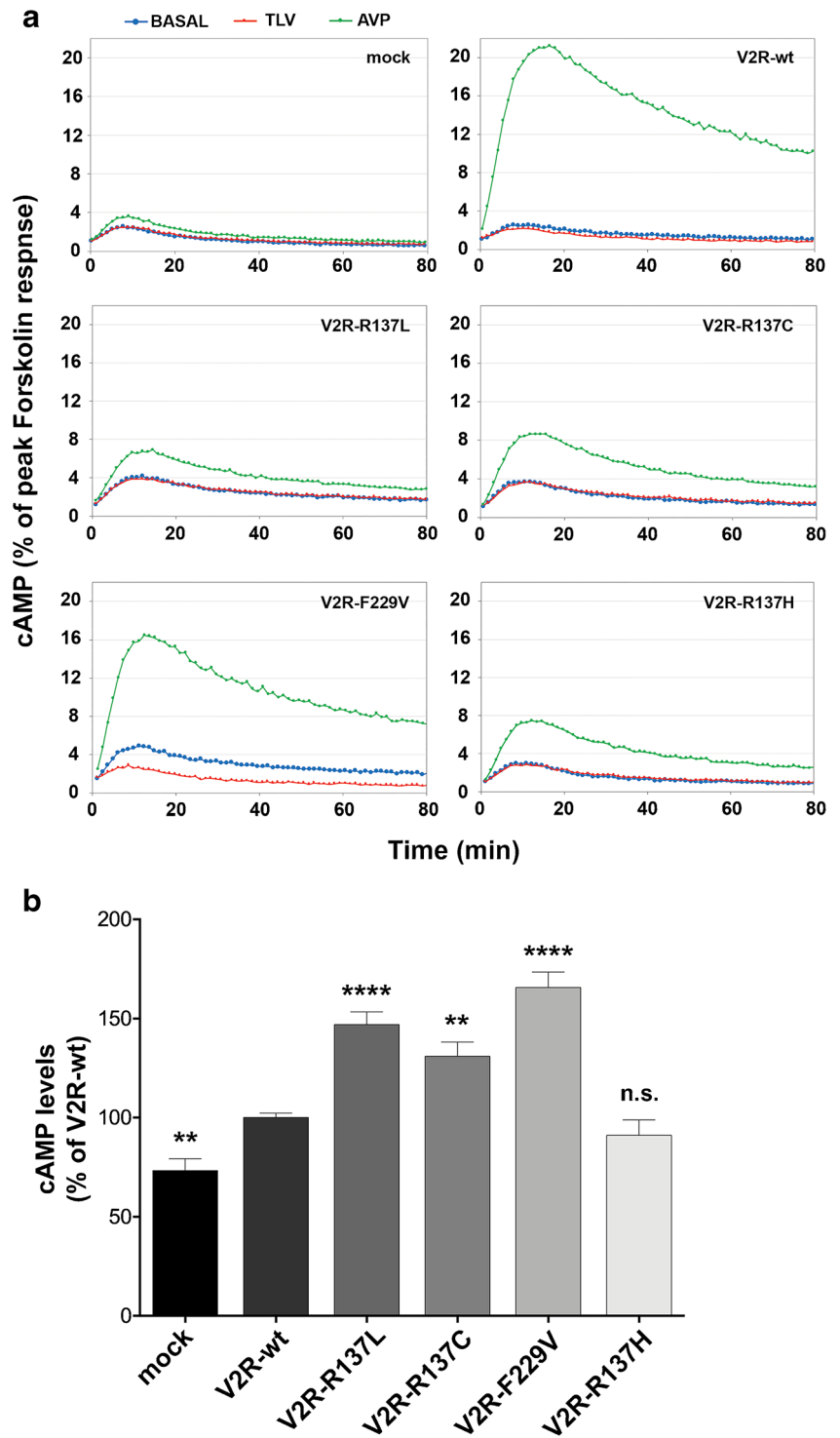
To detect cAMP levels in MCD4 cells with high sensitivity, we used the GloSensor technology, a luciferase-based biosensor which can detect real-time cAMP production in cells. The wild-type V2R and its mutants were transiently transfected in MCD4 cells stably expressing the GloSensor-22F, and luminescence was measured in cells co-expressing the biosensor and each receptor in basal conditions or after stimulation with different agents. As shown in Fig. 5, under basal conditions, cAMP levels (expressed as percentage of forskolin response) displayed almost a 2-fold increase in cells expressing the

constitutively active V2R mutants compared to cells not expressing recombinant receptors (mock). The rank order of receptor constitutive activity was  $F229V > R137L > R137C$ .

A small but significant increase in constitutive activity on cAMP production above mock cells was observed also in cells expressing the wild-type V2R. Considering that in our experiments the expression level of the F229V mutant was lower compared to that of other receptors (Fig. 1b), it is conceivable that its constitutive activity is much greater than that observed. Interestingly, stimulation with AVP induced a 4- to 5-fold increase in cAMP levels above basal in cells expressing either the wild-type V2R or its constitutively active F229V mutant, whereas agonist-induced cAMP production was less than 2-fold in cells expressing the R137 mutants (Fig. 5a). These results indicate that even in cells expressing the gain-of-function receptor F229V, known to be sensitive to AVP stimulation, the increased basal cAMP levels are far from those levels reached under stimulation with the physiological agonist AVP.

Overall, these findings are consistent with those from previous studies reporting increased basal cAMP production in cells expressing the constitutively active mutants R137L, R137C, and F229V [9, 12, 16, 17]. However, the degree of constitutive activity of each receptor mutant on cAMP response reported in previous studies was highly dependent on the methods used to detect cAMP. For example, in studies using CRE-luciferase reporter gene assay, basal cAMP production in cells expressing the R137L mutant ranged from 4- to 15-fold above the level of cells expressing the wild-type

**Fig. 5** cAMP levels in cells expressing the wild-type and mutated V2R. **a** cAMP levels in MCD4 cells detected with GloSensor technology. The wild-type V2R and its mutants were transiently transfected in MCD4 cells stably expressing the GloSensor-22F, and luminescence was measured in cells co-expressing the biosensor and each receptor under basal conditions and in the presence of 1  $\mu$ M AVP or tolvaptan (TLV). **b** The histogram shows constitutive cAMP response that was quantified as area under the curve of the tracings of GloSensor luminescence, measured in the absence of ligands, in cells expressing different receptors. Data were averaged ( $\pm$  s.e.m.) from 9 tracings and are expressed as percentage of the effect of forskolin measured in the same cells (\*\* $p < 0.01$ ; \*\*\*\* $p < 0.001$ ; n.s. not significant vs V2R-wt)



V2R [9, 12]. When basal cAMP production was measured using a FRET-based immunoassay, its levels in cells expressing the R137L mutant were only 2.5-fold greater than in cells expressing the wild-type receptor [17]. Using the GloSensor™ cAMP assay, a new generation technology to measure intracellular cAMP levels, we evaluated the cAMP levels in different cell types expressing R137L, R137C, and

F229V V2R active mutants compared to wild-type V2R expressing cells. As shown in Fig. 5 b, we obtained that cAMP levels in active mutants were significantly higher (R137L 147.0  $\pm$  6.5%; R137C 131.0  $\pm$  7.2%; F229V 165.7  $\pm$  7.7%;  $p < 0.01$ ) with respect to the wild-type V2R expressing cells (100.1  $\pm$  2.2%). In contrast, in cells expressing R137H inactive mutant, cAMP levels were not significantly different

( $91.05 \pm 7.8\%$ ) compared to cells expressing the wild-type V2R (Fig. 5b).

### Effect of tolvaptan on constitutive water reabsorption and cAMP production

It has been previously reported that inverse agonists, like satavaptan or tolvaptan, could inhibit the constitutive activity of the F229V mutant or of the L312S on cAMP response in vitro [12, 14], but not that of the R137L or R137C receptors [17]. Thus, we tested the effect of tolvaptan on basal water reabsorption in MCD4 cells expressing the constitutively active V2R receptor mutants.

As shown in Fig. 6, incubation with tolvaptan abolished the increase of basal water reabsorption in cells expressing the F229V mutant (F229V+TLV  $126.1 \pm 4.7\%$  vs F229V  $167.1 \pm 4.6\%$ ;  $p < 0.001$ ), whereas it did not have any effect on the constitutive activity of the R137L (R137L+TLV  $155.8 \pm 8.7\%$  vs R137L  $145.8 \pm 4.6\%$ ) or R137C mutants (R137C+TLV  $156.9 \pm 5.9\%$  vs R137C  $144.4 \pm 4.3\%$ ).

When tested on basal cAMP production, tolvaptan was able to inhibit the constitutive activity of the F229V mutant, but not that of the R137L or R137C receptors (Fig. 5a), in agreement with previous findings [12].

### AQP2 phosphorylation at Ser-256

Binding of AVP to the V2R leads to activation of protein kinase A-mediated phosphorylation of AQP2 at Ser-256

[22], and this phosphorylation event is crucial to increase water reabsorption in the renal collecting duct. To evaluate whether the expression of the active V2R mutants affects the basal levels of AQP2 phosphorylated at Ser-256 (pS256-AQP2), western blotting experiments using phosphospecific antibodies were performed. Interestingly, when normalized to total AQP2, basal pS256-AQP2 levels in cells expressing F229V were almost 2-fold higher than in cells expressing the wild-type V2R (F229V  $1.84 \pm 0.16$  a.u. vs V2R-wt  $1.00 \pm 0.04$  a.u.;  $p < 0.001$ ) (Fig. 7). This suggests that, in cells expressing the F229V mutant, constitutive AQP2 translocation to the apical membrane involves cAMP-dependent phosphorylation of Ser-256. In contrast, no significant changes in pS256-AQP2 levels were found in cells expressing either the R137L ( $0.81 \pm 0.20$  a.u.) or R137C ( $0.64 \pm 0.11$  a.u.) mutant. These findings might have different explanations. On one hand, it is possible that constitutive increase of cAMP levels induced by the R137 mutants, which was weaker compared to F229V (Fig. 5), is not sufficient to induce a measurable increase of pS256-AQP2. On the other hand, it is possible that both the R137L and R137C mutants activate additional signaling pathways underlying AQP2 regulation.

### Discussion

In this study, we have investigated some biochemical and functional features of V2R mutants carrying activating mutations (R137L, R137C, and F229V) which have been found in

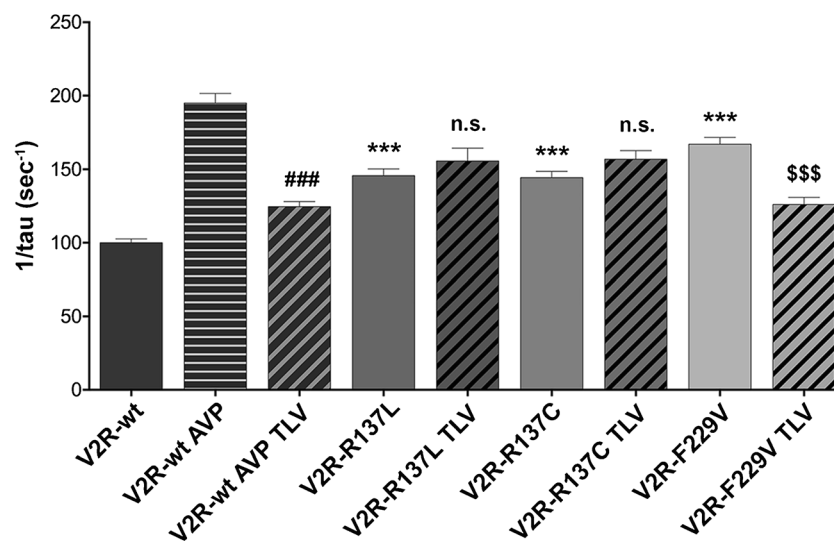


**Fig. 6** Effect of tolvaptan on water reabsorption. Osmotic permeability studies in MCD4 cells expressing the wild-type V2R and constitutive active R137L, R137C, and F229V were performed as reported in the “Materials and methods.” The temporal osmotic response is indicated as  $1/\tau$  ( $\text{s}^{-1}$ ). In cells expressing the wild-type V2R, tolvaptan was tested in cells stimulated with AVP. In cells expressing the active mutants,

tolvaptan was tested on unstimulated cells. The data, expressed as percentage of the level in cell expressing the wild-type V2R, are means ( $\pm$  s.e.m.) of 5 experiments. (\*\*\*)  $p < 0.001$  vs V2R-wt; (###)  $p < 0.001$  vs V2R-wt AVP; (\$\$\$)  $p < 0.001$  vs V2R-F229V; n.s. not significant vs V2R-R137L or V2R-R137C)



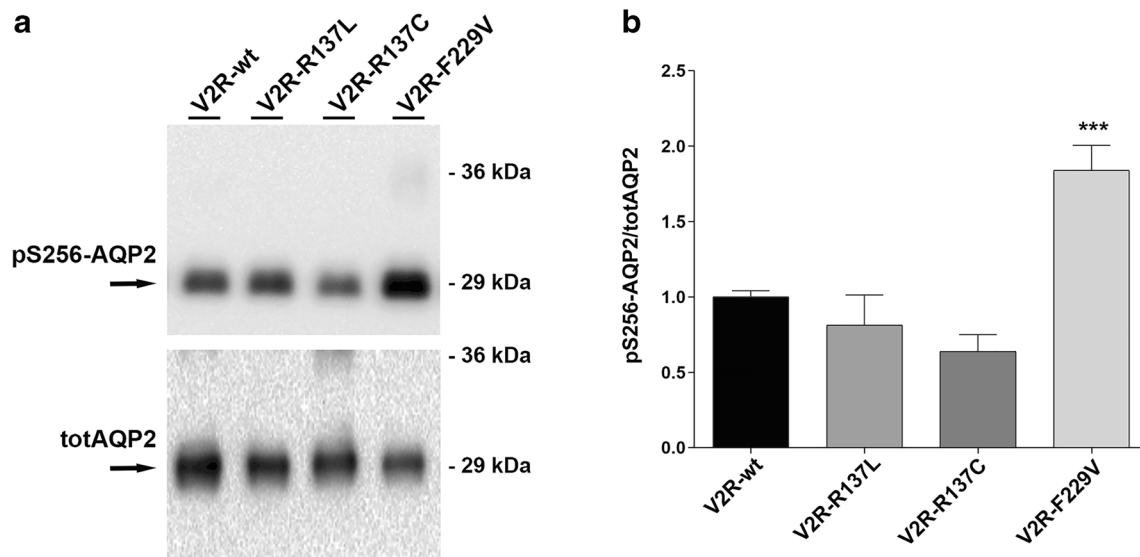


**Fig. 7** Phosphorylation of AQP2 on Ser-256 in cells expressing the wild-type and mutated V2R. **a** A representative western blot showing phosphorylation of AQP2 on Ser-256 (pS256-AQP2) in cells expressing the wild-type V2R or the constitutively R137L, R137C, and F229V in basal

patients suffering from NSIAD syndrome [9, 12]. In previous studies, the constitutive activity of the V2R mutants associated with NSIAD has been assessed as to their ability to induce agonist-independent increase of intracellular cAMP levels in recombinant cells [12, 14]. Whether and how this biochemical effect might be translated into the perturbation of water reabsorption, which is the pathological outcome of NSIAD, has not been explored so far. Our findings demonstrate a direct link between the activating mutations of the V2R and the alteration of water permeability in cells expressing V2R mutants (R137L, R137C, and F229V).

To characterize the functional consequences of V2R activating mutations, the R137L, R137C, and F229V receptors have been stably transfected in MCD4 cells, a cell line derived from mouse kidney collecting duct and overexpressing human AQP2, which represent a cell system close to the physiological environment where the V2R is expressed [19]. Cells expressing the constitutively active V2R mutants displayed increased basal water reabsorption (Fig. 4) which correlated with both agonist-independent translocation of AQP2 to the apical membrane (Fig. 3a, b) and the significant increase in cAMP production although to a different extent for each V2R mutant (Fig. 5).

Our findings show a good correlation between the effects of activating mutations of V2R on constitutive increase of cAMP levels (Fig. 5) and water permeability (Fig. 4) in MCD4 cells. However, the basal levels of AQP2 phosphorylated at Ser-256 (pS256-AQP2) were significantly increased in cells expressing the F229V mutant, but not in those expressing the R137L or R137C (Fig. 7). This observation suggests that, whereas the functional effects on AQP2 induced by

conditions. **b** Densitometric analysis of pS256-AQP2 bands normalized to total AQP2 bands (totAQP2) is reported in the histogram. The data, normalized to the level in cell expressing the wild-type V2R, are means ( $\pm$  s.e.m.) of five experiments (\*\* $p < 0.0001$  vs V2R-wt)

the F229V mutant are strictly cAMP-dependent, both the R137L and R137C mutants might activate additional signaling pathways underlying AQP2 regulation which have not been investigated in this study. This is in agreement with recent studies suggesting that multiple intracellular mechanisms can couple the V2R to AQP2 regulation [5, 25–27].

In agreement with what was reported in previous studies, our findings highlight some important differences between the F229V mutant and receptors carrying mutations of R137, in terms of cellular expression as well as functional behavior. Both the F229V mutant and receptors mutated at R137 displayed expression of the mature receptor form at the cell surface, but their level of cell surface expression was more than 50% lower compared to that of the wild-type V2R (Fig. 1b). However, whereas the F229V was mainly expressed at the cell surface, both active (R137L, R137C) and inactive (R137H) receptors mutated at R137 displayed marked retention in the intracellular compartments. This is in agreement with previous findings showing that either activating or inactivating mutations of R137 profoundly compromise cell surface expression of the V2R due to both impaired maturation and  $\beta$ -arrestin-mediated constitutive internalization [12, 14, 28].

With respect to the functional and pharmacological properties of the receptor mutants, the F229V receptor displayed greater constitutive activity, both at the level of water reabsorption (Fig. 4) and cAMP production (Fig. 5), compared to the R137L or R137C mutants. In addition, whereas the cAMP response mediated by the R137 mutants was only weakly stimulated by AVP, agonist-induced increase of cAMP mediated by F229V was similar to that of the wild-type V2R

(Fig. 5a). Finally, the constitutive activity of F229V on both water reabsorption and cAMP production was inhibited by tolvaptan, which behaved as an inverse agonist, whereas the active mutants carrying mutations of R137 were not responsive to this drug (Figs. 5 and 6).

Altogether, these findings suggest that the conformational changes induced by mutations of F229 and R137 result in different active “states” of the V2R [29]. In particular, the impaired capacity of the R137L and R137C mutants to respond to either AVP or tolvaptan suggests that mutations of R137 induce a “locked” active state of the V2R not responsive to pharmacological modulation. This is coherent with results from previous studies demonstrating that mutations of arginine in the highly conserved E/DRY motif, to which R137 belongs, can drive GPCRs into different “states” [30].

The different responsiveness to tolvaptan displayed by the constitutively active V2R mutants has important clinical implications. Treatment with currently available inverse agonists can be effective in NSIAD patients carrying the F229V, I130N, and L312S mutations, but not in those carrying mutations of R137 for whom standard treatment consists of fluid restriction and urea to increase urine osmolality. This difference in therapeutical indications implies that any novel mutation discovered in NSIAD cases should be subjected to extensive molecular investigations to assess the sensitivity of constitutive cAMP signaling to inverse agonists, as this information is of crucial diagnostic value for deciding optimal patient treatment. In contrast, the ideal theoretical pharmacological treatment of NSIAD associated with R137 or other, yet unknown, mutations unresponsive to current drugs will require to identify new inverse agonists selective for distinct active “states” of the mutated receptors.

NSIAD follows an X-linked pattern of transmission since the V2R gene is located on the long arm of the X chromosome (Xq28). Hyponatremia mainly occurs in male patients, but episodes of hyponatremia are not limited to hemizygous males as they can also affect heterozygous females. Hyponatremia can be severe and symptomatic, with the occurrence of seizures reported in several affected children. However, although harboring the same mutation, some patients were diagnosed in the neonatal period, while others were diagnosed later in life [15, 31]. This indicates variable expressivity of NSIAD both in male and female individuals, but it is not possible, so far, to establish a correlation between specific mutations and the severity of the clinical symptoms. At present, few patients affected by NSIAD have been identified, but the number of cases will increase once sequencing of the V2R gene will be done on more patients affected by inappropriate antidiuresis with undetectable AVP levels. Therefore, it will be important to fully characterize the molecular and functional properties of novel V2R mutations. An important implication of this study is to provide a useful assay system to assess the functional consequences of constitutively activating mutations of the

V2R on water permeability in kidney cells thus allowing to unequivocally identify the link between novel mutations and the perturbation of water balance which is the main pathogenic factor in NSIAD.

## Materials and methods

### Chemicals and reagents

All chemicals were purchased from Sigma (Sigma-Aldrich, Milan, Italy). Calcein-AM was bought from Molecular Probes (Life Technologies, Monza, Italy). Forskolin was purchased from Fermentek (Jerusalem, Israel). Cell culture media and FBS (fetal bovine serum) were from GIBCO (Life Technologies, Monza, Italy). Antibiotics were from Calbiochem. Super Signal® West Pico Chemiluminescent Substrate was from ThermoScientific (Rockford, USA) and used for the ChemiDoc System (Bio-Rad Laboratories, Milan, Italy).

### Antibodies

Vasopressin receptor (V2R) was detected using anti-c-Myc from Santa Cruz Biotechnologies (Tebu-Bio, Milan, Italy). Aquaporin (AQP2) was detected using a specific antibody (C-tail Ab) raised against a synthetic peptide corresponding to the last 15 C-terminal amino acids of human AQP2 [32]. AQP2-pS256 antibodies were kindly gifted by Peter Deen. Secondary goat anti-rabbit or goat anti-mouse horseradish peroxidase-coupled antibodies were obtained from Santa Cruz Biotechnologies (Tebu-Bio, Milan, Italy). Secondary goat anti-rabbit and anti-mouse Alexa 488 and 555 conjugate antibodies were from Molecular Probes (Eugene, OR, USA).

### Constructs

Human V2R wild type and mutants with c-Myc epitope in the N-terminal, expressed in pRK5 vector, were a gift from Prof. Michel Bouvier (Université de Montréal, Montréal, Quebec, Canada). Human c-Myc-tagged V2Rs (wild type and mutants) were fused to the N-terminal of Rluc (Renilla luciferase) by linking each receptor sequence without its stop codon to Rluc cDNA through a decanucleotide linker peptide (GGGGSGGGGS) and cloned into puromycin resistance retroviral expression vector pQCXIP (Clontech).

### Cell engineering and culture

Mouse cortical collecting duct MCD4 cells, stably transfected with the plasmid encoding the human AQP2 [33], were engineered to permanently express chimeric V2R-Rluc using the pantropic retroviral expression system by Clontech.

Briefly, recombinant retroviruses expressing receptor–Rluc fusion proteins were prepared by transfection of GP2-293 packaging cell with different retroviral vectors using polyethyleneimine linear MW 25,000 Da (PEI). Cells were allowed to increase the viral titer for 48 h before collecting the virus-containing supernatants. MCD4 cells were infected with the V2R-Rluc retroviruses in the presence of 8 µg/ml Polybrene for 24 h and selected under puromycin (1 µg/ml).

Then MCD4 were grown in a 1:1 mixture of Dulbecco's modified Eagle's medium and F-12 supplemented with 5% (v/v) fetal bovine serum, 1% (v/v) L-glutamine, 1% (v/v) non-essential amino acids and 1% penicillin/streptomycin, 5 µM dexamethasone, 400 µg/ml G418 (for AQP2 resistance), and 1 µg/ml puromycin (for V2R-Rluc resistance), in a humidified atmosphere of 5% CO<sub>2</sub> at 37 °C.

### Gel electrophoresis and immunoblotting

For immunoblotting studies, cells grown on 60-mm dishes were lysed in isolation medium (220 mM mannitol, 70 mM sucrose, 0.5 M EGTA pH 8.0, 0.5 M EDTA pH 8.0, 1 M Tris–HCl pH 7.4) in the presence of proteases (1 mM PMSF, 2 mg/ml leupeptin, and 2 mg/ml pepstatin A) and phosphatases (10 mM NaF and 1 mM sodium orthovanadate) inhibitors. The obtained lysates were potted at 1200×g. Nuclear and heavy organelle debris was removed by centrifugation at 2500×g for 15 min at 4 °C. The supernatants were then centrifuged at 21,000×g for 1 h. The pellets were collected and resuspended in isolation medium and used for immunoblotting studies.

Proteins were separated on 8% Bis-Tris acrylamide gels under reducing conditions. Protein bands were electrophoretically transferred onto Immobilon-P membranes (Millipore Corporate Headquarters, Billerica, USA) for western blot analysis, blocked in TBS–Tween-20 containing 3% bovine serum albumin (BSA) and incubated with primary antibodies O/N. Anti-AQP2 (pre-C-tail Ab) and anti-AQP2-pS256 were used at 1:1000 dilution; anti-c-Myc was used at 1:100 dilution. Immunoreactive bands were detected with secondary goat anti-mouse horseradish peroxidase–coupled antibodies obtained from Santa Cruz Biotechnologies (Tebu-Bio, Milan, Italy). Membranes were developed using Super Signal® West Pico Chemiluminescent Substrate (ThermoScientific, Rockford, USA) with the ChemiDoc System (Bio-Rad Laboratories, Milan, Italy). Densitometry analysis was performed using Image Lab (Bio-Rad Laboratories, Milan, Italy). Data are summarized in histograms by using GraphPad Prism (GraphPad Software, San Diego, CA).

### Confocal microscopy

For confocal microscopy, cells were grown on cell culture filters (Transwell PET inserts), and in order to induce cell polarization, 24 h before the experiment, cells were cultured

in Opti-MEM (ThermoScientific, Rockford, USA), treated with different agents, and fixed for 20 min with 4% paraformaldehyde in PBS. Samples were permeabilized with 0.1% Triton X-100 in PBS for 5 min, blocked with 1% BSA–PBS added with 0.1% SDS for 45 min, and incubated with a 1:3000 dilution of AQP2 antibody or 1:100 dilution of c-Myc antibody for 2 h. After washing three times with 1% BSA–PBS, samples were incubated with 1:1000 diluted goat anti-rabbit or anti-mouse antibodies coupled to Alexa 488 or 555 in 1% BSA–PBS for 1 h. Next, cells were rinsed three times with PBS and mounted on glass slides with Mowiol. Images were obtained with a confocal laser scanning fluorescence microscope Leica TCS SP2 (Leica Microsystems, Heerbrugg, Switzerland).

### Measurement of total intrinsic luminescence of receptors

To assess total receptor expression in whole cell extracts, cells grown in plastic dishes were detached using PBS containing 1 mM EDTA and pelleted at 1000×g. The pellets were resuspended in Tris/HCl 10 mM pH 7.4, sonicated (20 s, 60 V) in ice, and stored at –80 °C. The amount of proteins in each extract was measured by Lowry's method. Luminescence was recorded in 96-well white plastic plates (Packard OptiPlate) using a plate luminometer (VICTOR Light, PerkinElmer) equipped with two independent automatic injectors.

In each assay, 7 duplicate serial dilutions of each cell extract (0.15–10 µg of protein) in PBS supplemented with Ca<sup>2+</sup> Mg<sup>2+</sup> were counted in the luminometer using an automated protocol; 0.5 µM (final) of coelenterazine was automatically injected to each sample, and after a delay of 2 s, total light emission was counted at 0.5-s intervals for 5-fold. Integrated photon counts were plotted as a function of protein concentration, and the luminescence (counts/µg of protein) of the extract was computed by linear regression of the data.

### Cell surface expression of receptors

To measure surface expression of wild-type and mutated V2R, we developed a cell-based ELISA (enzyme-linked immunosorbent assay). Cells were plated in 96-well white plastic plates (about 5000 cells/well) in 100 µl of medium without antibiotics and then exposed to various experimental treatments. After 24 h, cell layers were fixed in equal volume (100 µl) of paraformaldehyde 4% in PBS to the wells containing culture media for 10 min at room temperature (RT) and washed 3× with 300 µl of PBS. Nonspecific binding was blocked for 1 h at RT with 5% (w/v) nonfat dry milk dissolved in PBS. After washing again 3× with PBS, the wells were exposed to the antibody anti-c-Myc AP conjugated (1:10,000) in 5% (w/v) nonfat dry milk in PBS (100 µl) for an additional hour at RT. Extensive washing (5×) with PBS

was followed by the addition of 50  $\mu\text{l}$ /well of the chemiluminescent substrate VisiGlo AP. The luminescence was recorded in the plate luminometer for about 4 h. Photon counts were integrated in function of time, as area under the curve.

Cell monolayers were quantified by Cell Counting Kit-8 (Biotool), according to the manufacturer's protocol, measuring absorbance at 450 nm.

### Cell surface biotinylation of AQP2

Biotinylation was carried out according to the manufacturer's protocol (Pierce) with some adaptations. MCD4 cells were cultured on 6-well filters in DMEM for 4 days and washed thoroughly with ice-cold coupling buffer (0.1 M sodium phosphate and 0.15 M NaCl [pH 7.2]) before being subjected to oxidation with  $\text{Na}^+$  metaperiodate (20 mM) in coupling buffer for 30 min on ice in the dark. After three rounds of washing with coupling buffer, cell surface glycoproteins were labeled with 5 mM biocytin hydrazide (EZ-Link Pierce) for 30 min. After removing the biotinylation buffer, cells were incubated with quenching solution (50 mM  $\text{NH}_4\text{Cl}$  in PBS at pH 7.2) for 5 min and washed three times with coupling buffer. Cells were solubilized with lysis buffer (1% Triton X-100 and 0.01% SDS in PBS) supplemented with 2 mg/ml pepstatin A, 2 mg/ml leupeptin, and 2 mM PMSF for 30 min. The lysates were homogenized using an ultrasonic homogenizer at 40 Hz for 20 s and centrifuged at  $12,000\times g$  for 20 min. An aliquot of the supernatants (20 ml) was diluted in Laemmli's buffer, whereas the remaining biotinylated proteins were pulled down with immobilized streptavidin beads. The complexes were washed three times with wash buffer (Triton X-100 0.5% and SDS 0.01% in PBS), denatured in Laemmli's buffer for 10 min at 90 °C and 400 rpm, and analyzed by SDS-PAGE and immunoblotting using anti-AQP2 antibodies.

### Water permeability assay

Osmotic water permeability was measured by video imaging experiments as previously described [34]. Briefly, MCD4 cells were grown on 40 mm glass coverslips and loaded with 10  $\mu\text{M}$  membrane-permeable Calcein-AM for 45 min at 37 °C, 5%  $\text{CO}_2$  in DMEM. Cells were left under basal condition or stimulated with 1  $\mu\text{M}$  dDAVP for 30 min or treated with 10 nM tolvaptan for 45 min. The coverslips with dye-loaded cells were mounted in a perfusion chamber (FCS2 Closed Chamber System, Biopetech, Butler, USA) and measurements were performed, under basal conditions, using an inverted microscope (Nikon Eclipse TE2000-S microscope) equipped for single-cell fluorescence measurements and imaging analysis. The Calcein-AM-loaded sample was excited at 490 nm. Fluorescence measurements, following isosmotic (140 mM NaCl, 5 mM KCl, 1 mM  $\text{MgCl}_2$ , 1 mM  $\text{CaCl}_2$ , 10 mM HEPES sulfonic acid, 5 mM glucose, pH 7.4) or

hyperosmotic (isosmotic solution added with 135 mM mannitol) solutions, were carried out using MetaFluor software (Molecular Devices, MDS Analytical Technologies, Toronto, Canada). Exposure to a hyperosmotic solution causes water exit from cells with a consequent cell shrinkage resulting in Calcein-AM-increased concentration and self-quenching. The speed of decrease in fluorescence intensity is proportional to the speed of water efflux and, indirectly, to the water permeability through AQP2 water channels. The time course of cell shrinkage was measured as time constant ( $K_i$ ,  $\text{s}^{-1}$ ).

### cAMP assay

MCD4 cells stably expressing GloSensor-22F and transiently expressing V2R wild-type and mutant-Rluc were seeded in 96-well white plates at a density of  $20 \times 10^3$  cells/well 24 h after transfection of receptors and 24 h before performing the experiment. One hour before the assay, cells were washed once with PBS and incubated in PBS + 25 mM glucose in the presence of 2 mM luciferin in a total volume of 50  $\mu\text{l}$ . After 60 min, ligands were added with 100  $\mu\text{M}$  (final) rolipram in a total volume of 100  $\mu\text{l}$ /well and the plate was counted in a plate luminometer. Luminescence from each well was counted every 30 s with 0.5 s integration time for about 80 min. Ligands were diluted in 0.1% BSA in PBS and rolipram in PBS added with 25 mM glucose. cAMP response was determined as area under the luminescence-time curves. Resulting values for each ligand were corrected either with respect to the forskolin (100  $\mu\text{M}$ ) response obtained in parallel experiments.

### Statistical analysis

Nonparametric one-way ANOVA followed by a comparison with column control was used for all statistical analysis. All values are expressed as means  $\pm$  s.e.m. A difference of  $p < 0.05$  was considered statistically significant.

**Acknowledgments** We are grateful to Dr. Paola Molinari (Istituto Superiore di Sanità, Rome) for her advice in signal transduction experiments and Prof. Francesca Fanelli (University of Modena-Reggio Emilia) for helpful discussions. We thank Prof. Michel Bouvier (University of Montreal, Canada) for providing the cDNA of the V2 receptors.

**Funding information** The financial support of Telethon - Italy (Grant Number GGP13227) is gratefully acknowledged. Marianna Ranieri is a postdoctoral research fellow supported by "Intervento cofinanziato dal Fondo di Sviluppo e Coesione 2007-2013-APQ Ricerca Regione Puglia, Programma Regionale a Sostegno della Specializzazione Intelligente e della Sostenibilità Sociale ed Ambientale-FutureInResearch."

### Compliance with ethical standards

**Conflict of interest** The authors declare that they have no conflict of interest.



## References

- Birnbaumer M (2000) Vasopressin receptors. *Trends Endocrinol Metab* 11:406–410
- Bouley R, Hasler U, Lu HA, Nunes P, Brown D (2008) Bypassing vasopressin receptor signaling pathways in nephrogenic diabetes insipidus. *Semin Nephrol* 28:266–278. <https://doi.org/10.1016/j.semnephrol.2008.03.010>
- Boone M, Deen PM (2008) Physiology and pathophysiology of the vasopressin-regulated renal water reabsorption. *Pflugers Arch* 456:1005–1024. <https://doi.org/10.1007/s00424-008-0498-1>
- Olesen ET, Moeller HB, Assentoft M, MacAulay N, Fenton RA (2016) The vasopressin type 2 receptor and prostaglandin receptors EP2 and EP4 can increase aquaporin-2 plasma membrane targeting through a cAMP-independent pathway. *Am J Physiol Renal Physiol* 311:F935–F944. <https://doi.org/10.1152/ajprenal.00559.2015>
- Tamma G, Lasorsa D, Trimpert C, Ranieri M, Di Mise A, Mola MG, Mastrofrancesco L, Devuyt O, Svelto M, Deen PM, Valenti G (2014) A protein kinase A-independent pathway controlling aquaporin 2 trafficking as a possible cause for the syndrome of inappropriate antidiuresis associated with polycystic kidney disease 1 haploinsufficiency. *J Am Soc Nephrol* 25:2241–2253. <https://doi.org/10.1681/asn.2013111234>
- Bichet DG (2006) Diabètes insipides néphrogéniques (Nephrogenic diabetes insipidus). *Nephrol Ther* 2:387–404. <https://doi.org/10.1016/j.nephro.2006.07.010>
- Morello JP, Bichet DG (2001) Nephrogenic diabetes insipidus. *Annu Rev Physiol* 63:607–630. <https://doi.org/10.1146/annurev.physiol.63.1.607>
- Ranieri M, Di Mise A, Tamma G, Valenti G (2019) Vasopressin-aquaporin-2 pathway: recent advances in understanding water balance disorders. *F1000Research* 8:8. <https://doi.org/10.12688/f1000research.16654.1>
- Feldman BJ, Rosenthal SM, Vargas GA, Fenwick RG, Huang EA, Matsuda-Abedini M, Lustig RH, Mathias RS, Portale AA, Miller WL, Gitelman SE (2005) Nephrogenic syndrome of inappropriate antidiuresis. *N Engl J Med* 352:1884–1890. <https://doi.org/10.1056/NEJMoa042743>
- Bartter FC, Schwartz WB (1967) The syndrome of inappropriate secretion of antidiuretic hormone. *Am J Med* 42:790–806
- Rosenthal W, Seibold A, Antaramian A, Gilbert S, Birnbaumer M, Bichet DG, Arthus MF, Loneragan M (1994) Mutations in the vasopressin V2 receptor gene in families with nephrogenic diabetes insipidus and functional expression of the Q-2 mutant. *Cell Mol Biol (Noisy-le-Grand)* 40:429–436
- Carpentier E, Greenbaum LA, Rochdi D, Abrol R, Goddard WA 3rd, Bichet DG, Bouvier M (2012) Identification and characterization of an activating F229V substitution in the V2 vasopressin receptor in an infant with NSIAD. *J Am Soc Nephrol* 23:1635–1640. <https://doi.org/10.1681/asn.2012010077>
- Erdelyi LS, Mann WA, Morris-Rosendahl DJ, Gross U, Nagel M, Varnai P, Balla A, Hunyady L (2015) Mutation in the V2 vasopressin receptor gene, AVPR2, causes nephrogenic syndrome of inappropriate diuresis. *Kidney Int* 88:1070–1078. <https://doi.org/10.1038/ki.2015.181>
- Tiulpakov A, White CW, Abhayawardana RS, See HB, Chan AS, Seeber RM, Heng JI, Dedov I, Pavlos NJ, Pflieger KD (2016) Mutations of vasopressin receptor 2 including novel L312S have differential effects on trafficking. *Mol Endocrinol* 30:889–904. <https://doi.org/10.1210/me.2016-1002>
- Decaux G, Vanderghenst F, Bouko Y, Parma J, Vassart G, Vilain C (2007) Nephrogenic syndrome of inappropriate antidiuresis in adults: high phenotypic variability in men and women from a large pedigree. *J Am Soc Nephrol* 18:606–612. <https://doi.org/10.1681/asn.2006090987>
- Rochdi MD, Vargas GA, Carpentier E, Oligny-Longpre G, Chen S, Kovoora A, Gitelman SE, Rosenthal SM, von Zastrow M, Bouvier M (2010) Functional characterization of vasopressin type 2 receptor substitutions (R137H/C/L) leading to nephrogenic diabetes insipidus and nephrogenic syndrome of inappropriate antidiuresis: implications for treatments. *Mol Pharmacol* 77:836–845. <https://doi.org/10.1124/mol.109.061804>
- Tenenbaum J, Ayoub MA, Perkovska S, Adra-Delenne AL, Mendre C, Ranchin B, Bricca G, Geelen G, Mouillac B, Durroux T, Morin D (2009) The constitutively active V2 receptor mutants conferring NSIAD are weakly sensitive to agonist and antagonist regulation. *PLoS One* 4:e8383. <https://doi.org/10.1371/journal.pone.0008383>
- Kocan M, See HB, Sampaio NG, Eidne KA, Feldman BJ, Pflieger KD (2009) Agonist-independent interactions between beta-arrestins and mutant vasopressin type II receptors associated with nephrogenic syndrome of inappropriate antidiuresis. *Mol. Endocrinol (Baltimore, Md)* 23:559–571. <https://doi.org/10.1210/me.2008-0321>
- Iolascon A, Aglio V, Tamma G, D'Apolito M, Addabbo F, Procinio G, Simonetti MC, Montini G, Gesualdo L, Debler EW, Svelto M, Valenti G (2007) Characterization of two novel missense mutations in the AQP2 gene causing nephrogenic diabetes insipidus. *Nephron Physiol* 105:p33–p41. <https://doi.org/10.1159/000098136>
- Jung HJ, Kwon TH (2016) Molecular mechanisms regulating aquaporin-2 in kidney collecting duct. *Am J Physiol Renal Physiol* 311:F1318–F1328. <https://doi.org/10.1152/ajprenal.00485.2016>
- Kwon TH, Frokiaer J, Nielsen S (2013) Regulation of aquaporin-2 in the kidney: a molecular mechanism of body-water homeostasis. *Kidney Res Clin Pract* 32:96–102. <https://doi.org/10.1016/j.krcp.2013.07.005>
- Nedvetsky PI, Tamma G, Beulshausen S, Valenti G, Rosenthal W, Klusmann E (2009) Regulation of aquaporin-2 trafficking. *Handb Exp Pharmacol*:133–157. [https://doi.org/10.1007/978-3-540-79885-9\\_6](https://doi.org/10.1007/978-3-540-79885-9_6)
- Noda Y, Sasaki S (2006) Regulation of aquaporin-2 trafficking and its binding protein complex. *Biochim Biophys Acta* 1758:1117–1125. <https://doi.org/10.1016/j.bbamem.2006.03.004>
- Valenti G, Procinio G, Tamma G, Carmosino M, Svelto M (2005) Minireview: Aquaporin 2 trafficking. *Endocrinology* 146:5063–5070. <https://doi.org/10.1210/en.2005-0868>
- Ando F, Sohara E, Morimoto T, Yui N, Nomura N, Kikuchi E, Takahashi D, Mori T, Vandewalle A, Rai T, Sasaki S, Kondo Y, Uchida S (2016) Wnt5a induces renal AQP2 expression by activating calcineurin signalling pathway. *Nat Commun* 7:13636. <https://doi.org/10.1038/ncomms13636>
- Cheung PW, Terlouw A, Janssen SA, Brown D, Bouley R (2019) Inhibition of non-receptor tyrosine kinase Src induces phosphoserine 256-independent aquaporin-2 membrane accumulation. *J Physiol* 597:1627–1642. <https://doi.org/10.1113/jp277024>
- Olesen ET, Fenton RA (2017) Aquaporin-2 membrane targeting: still a conundrum. *Am J Physiol Renal Physiol* 312:F744–F747. <https://doi.org/10.1152/ajprenal.00010.2017>
- Barak LS, Oakley RH, Laporte SA, Caron MG (2001) Constitutive arrestin-mediated desensitization of a human vasopressin receptor mutant associated with nephrogenic diabetes insipidus. *Proc Natl Acad Sci U S A* 98:93–98. <https://doi.org/10.1073/pnas.0111303698>
- Costa T, Cotecchia S (2005) Historical review: negative efficacy and the constitutive activity of G-protein-coupled receptors. *Trends Pharmacol Sci* 26:618–624. <https://doi.org/10.1016/j.tips.2005.10.009>
- Scheer A, Costa T, Fanelli F, De Benedetti PG, Mhaouty-Kodja S, Abuin L, Nenniger-Tosato M, Cotecchia S (2000) Mutational

- analysis of the highly conserved arginine within the Glu/Asp-Arg-Tyr motif of the alpha(1b)-adrenergic receptor: effects on receptor isomerization and activation. *Mol Pharmacol* 57:219–231
31. Steinberg EA, Moss M, Buchanan CL, Goebel J (2018) Adherence in pediatric kidney transplant recipients: solutions for the system. *Pediatr Nephrol* 33:361–372. <https://doi.org/10.1007/s00467-017-3637-0>
  32. Tamma G, Procino G, Strafino A, Bononi E, Meyer G, Paulmichl M, Formoso V, Svelto M, Valenti G (2007) Hypotonicity induces aquaporin-2 internalization and cytosol-to-membrane translocation of ICln in renal cells. *Endocrinology* 148:1118–1130. <https://doi.org/10.1210/en.2006-1277>
  33. Procino G, Barbieri C, Tamma G, De Benedictis L, Pessin JE, Svelto M, Valenti G (2008) AQP2 exocytosis in the renal collecting duct—involvement of SNARE isoforms and the regulatory role of Munc18b. *J Cell Sci* 121:2097–2106. <https://doi.org/10.1242/jcs.022210>
  34. Ranieri M, Tamma G, Di Mise A, Russo A, Centrone M, Svelto M, Calamita G, Valenti G (2015) Negative feedback from CaSR signaling to aquaporin-2 sensitizes vasopressin to extracellular Ca<sup>2+</sup>. *J Cell Sci* 128:2350–2360. <https://doi.org/10.1242/jcs.168096>

**Publisher's note** Springer Nature remains neutral with regard to jurisdictional claims in published maps and institutional affiliations.